

Assessment of Distinct Tower Structures Impact on the Transient Behavior for Overhead Lines

A. C. S. Lima, J. P. L. Salvador, A. P. C. Magalhães, M. T. Correia de Barros

Abstract—For actual overhead circuits it is likely that distinct tower profiles are needed depending on the terrain involved. In this work, we consider a very hilly terrain where an overhead line is expected to be built. This demands the usage of several different types of structures leading to a rather complex network. A compact formulation of the equivalent nodal admittance is proposed based on the concept of the chain matrix. Three alternative approximations based on the average impedance and admittance of line segments and an uniform configuration, i.e., a single type of tower for the whole circuit, are also investigated. Frequency domain analysis is carried out to evaluate the accuracy of the simplified approaches. Results indicate that three possibilities lead to similar behavior of the nodal admittance matrix with the simplified approaches presenting some small deviations around the minima. To investigate further the impact of those small deviations simple test cases based on the time response obtained via the Numerical Laplace Transform (NLT) are considered. These results indicate that the small deviation have noticeable impact in the time-responses.

Keywords—Frequency dependent parameters, Overhead Lines, Tower Profiles.

I. INTRODUCTION

THE accurate representation of overhead lines has been a subject of intense interest. Since the pioneering work in the frequency domain in 1960s, a topic of special importance is the inclusion of the frequency dependence of the per unit length parameters in the line modeling [1,2]. In the time domain simulations, the first approaches of frequency dependent line models used modal domain with real and constant transformation matrix [3,4]. It was only in the mid to late 1990s that models using full phase coordinates were proposed, i.e., including all the aspects that contribute to the frequency dependence of a line model [5]–[13]. Independently of the domain considered, a key issue for the realization of the frequency dependence is an accurate representation of the

conductors spatial arrangement. In all these references, a single tower profile is used in the test cases. However, for actual overhead circuits it is likely that distinct tower profiles are needed depending on the considered terrain.

In this work, we consider an actual very hilly terrain where an overhead line is expected to be built. This demands the usage of several different types of structures leading to a nonuniform overhead line. There are a number of procedures to do so. One may consider a cascade of conventional full phase line models, where each section with the same type of tower is represented by its own model, or alternatively, one may treat the whole circuit as a frequency dependent network equivalent (FDNE) obtained via the chain matrix [14] which can then be implemented in time-domain simulations as rational approximation [15,16] or as polynomials in frequency domain [17].

In this paper, we propose to compare a more complete formulation, based on FDNE obtained via the chain matrix, with approximated approaches. First one considers the calculation of impedances and admittances as an average weighted by the line segment length which each tower is applied. Other approximation is obtained where a single tower that are dominant in the circuit, i.e., appears in a greater part of the circuit, is considered. We show the results for two different towers that have closest participation in the circuit.

The paper is organized as follows. A description of the circuit involved in the analysis is presented in Section II. Section III presents the procedure for obtaining the transfer admittance between the sending and receiving ends of the line and the behavior and fitting of the equivalent nodal admittance matrix. The evaluation of the time responses of the equivalent system as well as the detailed one are shown in Section IV. The presentation of the main conclusions of the paper is shown in Section V.

II. NETWORK DESCRIPTION

The circuit considered for this analysis consists of 500 kV overhead line, with a bundle of four sub-conductors and a total length of 215 km. An optimized configuration was obtained using a procedure to maximize the natural power of the circuit, regarding the voltage and bundle sets, similar to the ones described in [18], for an Ultra High Voltage with 2500 km in length, and in [19] for the design of a 420 kV, 865 km, 900 MW circuit. The conductors arrangement is depicted in Fig. 1 considering average heights and a plane terrain. Phase conductors have a 26.53 mm diameter, ground wires are 3/8” EHS. However, this arrangement is only feasible in a plane

This work was supported in part by a funding from INERGE (Instituto Nacional de Energia Elétrica), CAPES (Coordenação de Aperfeiçoamento de Pessoal de Nível Superior), CNPq (Brazilian National Council for Scientific and Technological Development), FAPEMIG (Fundação de Amparo a Pesquisa do Estado de Minas Gerais) and FAPERJ (Fundação Carlos Chagas de Amparo à Pesquisa do Estado do Rio de Janeiro).

A. C. S. Lima is with Electrical Engineering Department, Federal University of Rio de Janeiro, COPPE/UFRJ, Rio de Janeiro, Brazil; J. P. L. Salvador is with the Federal Center of Technological Education “Celso Suckow da Fonseca”, CEFET/RJ, Angra dos Reis, Brazil; A. P. C. Magalhães is post-doc researcher at the Federal University of Rio de Janeiro, with INCT-CAPES/BRASIL support – Finance Code 001; M. T. Correia de Barros is with Instituto Superior Técnico, Universidade de Lisboa, Lisbon, Portugal. (e-mails: joao.salvador@cefet-rj.br, apcm@dee.ufrj.br, acsl@dee.ufrj.br, teresa.correiaedebarras@tecnico.ulisboa.pt).

Paper submitted to the International Conference on Power Systems Transients (IPST2019) in Perpignan, France June 16-20, 2019.

terrain, once a cross-rope configuration is expected to be used. Nevertheless, when hilly terrain is considered, self-supporting structures are needed.

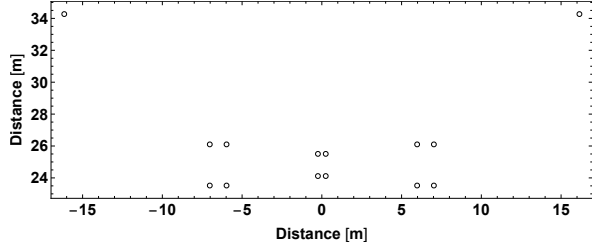
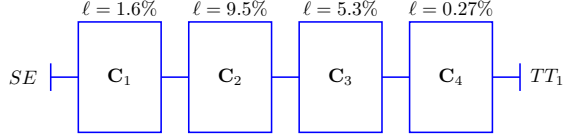
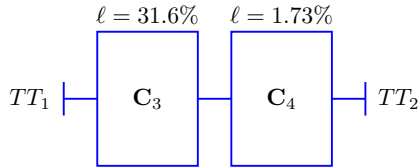


Fig. 1. Conductors arrangement for the “basic configuration”.

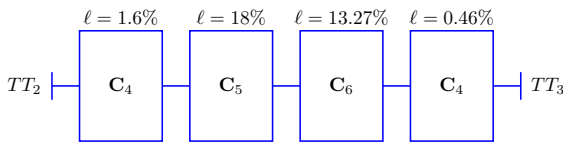
Six types of tower types were considered in order to attend terrain conditions. Fig. 2 depicts how the structures are positioned throughout the whole line. In this figure, C_i stands for “Configuration i ” of the arrangement of the sub-conductors. In appendix, we detail the characteristics of these bundle configurations. The “basic configuration” is represented by C_5 in Fig. 2. Structures C_1 to C_4 are self-supporting while C_5 and C_6 are cross-rope, due to the profile of the terrain, and that is the main reason for the several distinct types of towers.



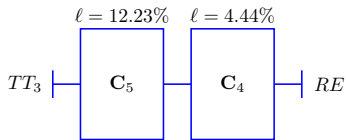
(a) 1st part of the circuit: from the sending end (SE) to the first transposition tower (TT_1)



(b) 2nd part of the circuit: from the first transposition tower (TT_1) to the second one (TT_2)



(c) 3rd part of the circuit: from the second transposition tower (TT_2) to the third one (TT_3)



(d) 4th part of the circuit: from the third one (TT_3) to the receiving end (RE)

Fig. 2. Tower structures along the overhead circuit.

III. FREQUENCY DOMAIN ANALYSIS

A. Complete Model

A rather compact formulation is possible if the chain matrix is considered [14]. This procedure consists in obtaining the transfer admittance between the sending and receiving ends of the line and is rather straightforward:

- I. To obtain \mathbf{Y}_{n_i} the nodal admittance for each configuration C_i given by

$$\mathbf{Y}_{n_i} = \begin{bmatrix} \mathbf{Y}_{s_i} & \mathbf{Y}_{m_i} \\ \mathbf{Y}_{m_i} & \mathbf{Y}_{s_i} \end{bmatrix} \quad (1)$$

where the block matrices in (1) are defined as

$$\mathbf{Y}_{s_i} = \mathbf{Y}_c (\mathbf{I} + \mathbf{H}^2) (\mathbf{I} - \mathbf{H}^2)^{-1} \quad (2)$$

$$\mathbf{Y}_{m_i} = -2\mathbf{Y}_c (\mathbf{I} - \mathbf{H}^2)^{-1} \quad (3)$$

where \mathbf{I} is a $n \times n$ identity matrix, with n being the number of conductors involved, $\mathbf{Y}_{c_i} = \mathbf{Z}^{-1} \sqrt{\mathbf{Z}\mathbf{Y}}$ is the characteristic admittance matrix, $\mathbf{H} = \exp(-\ell \sqrt{\mathbf{Z}\mathbf{Y}})$ is the propagation matrix also known as voltage deformation matrix and ℓ is the line length of configuration C_i . The characteristic admittance and the propagation matrices can be obtained using modal decomposition or Schur decomposition. This allows for a phase-domain approach without resorting to modal decomposition [20].

- II. To convert each \mathbf{Y}_{n_i} to a transfer function \mathbf{Q}_i . This can be achieved considering that

$$\mathbf{Q}_i = \begin{bmatrix} \mathbf{A} & \mathbf{B} \\ \mathbf{C} & \mathbf{D} \end{bmatrix} = \begin{bmatrix} -\mathbf{Y}_{m_i}^{-1} \mathbf{Y}_{s_i} & -\mathbf{Y}_{m_i}^{-1} \\ \mathbf{Y}_{m_i} - \mathbf{Y}_{s_i} \mathbf{Y}_{m_i}^{-1} \mathbf{Y}_{s_i} & \mathbf{Y}_{s_i} \mathbf{Y}_{m_i}^{-1} \end{bmatrix} \quad (4)$$

- III. To cascade each \mathbf{Q}_i , but we should consider the transposition scheme. This can be achieved by a rotation matrix \mathbf{R} defined as

$$\mathbf{R} = \begin{bmatrix} \mathbf{R}_1 & \mathbf{0} \\ \mathbf{0} & \mathbf{R}_1 \end{bmatrix} \quad (5)$$

with \mathbf{R}_1 given by

$$\mathbf{R}_1 = \begin{bmatrix} 0 & 1 & 0 \\ 0 & 0 & 1 \\ 1 & 0 & 0 \end{bmatrix} \quad (6)$$

- IV. To assemble the transfer matrix for the whole line

$$\mathbf{Q}_{eq} = \mathbf{Q}_I \cdot \mathbf{R} \cdot \mathbf{Q}_{II} \cdot \mathbf{R} \cdot \mathbf{Q}_{III} \cdot \mathbf{R} \cdot \mathbf{Q}_{IV} \quad (7)$$

where

$$\mathbf{Q}_I = \mathbf{Q}_1 \cdot \mathbf{Q}_2 \cdot \mathbf{Q}_3 \cdot \mathbf{Q}_4 \quad \mathbf{Q}_{II} = \mathbf{Q}_3 \cdot \mathbf{Q}_4 \quad (8)$$

$$\mathbf{Q}_{III} = \mathbf{Q}_4 \cdot \mathbf{Q}_5 \cdot \mathbf{Q}_6 \cdot \mathbf{Q}_4 \quad \mathbf{Q}_{IV} = \mathbf{Q}_5 \cdot \mathbf{Q}_4 \quad (9)$$

and

$$\mathbf{Q}_{eq} = \begin{bmatrix} \mathbf{A}_{eq} & \mathbf{B}_{eq} \\ \mathbf{C}_{eq} & \mathbf{A}_{eq} \end{bmatrix} \quad (10)$$

- V. To obtain the equivalent nodal admittance matrix from (10)

$$\mathbf{Y}_{n_{eq}} = \begin{bmatrix} \mathbf{D}_{eq} \mathbf{B}_{eq}^{-1} & \mathbf{C}_{eq} - \mathbf{D}_{eq} \mathbf{B}_{eq}^{-1} \mathbf{A}_{eq} \\ -\mathbf{B}_{eq}^{-1} & -\mathbf{B}_{eq}^{-1} \mathbf{A}_{eq} \end{bmatrix} \quad (11)$$

B. Considering Average Impedances and Admittances

A simpler approach that is often used for practical consulting projects is to build the nodal admittance matrix from average values of the per unit length impedance Z_i and admittance Y_i obtained from each tower profile and weighted with corresponding length portions of the whole line. From Fig. 2, we get the percentage value each configuration corresponds to and we summarize it in Table I, with ℓ the same as before.

TABLE I
PER-UNIT LENGTHS OF LINE SEGMENTS AND RESPECTIVE CONFIGURATIONS.

ℓ_1	ℓ_2	ℓ_3	ℓ_4	ℓ_5	ℓ_6
0.0160 ℓ	0.0950 ℓ	0.3690 ℓ	0.0850 ℓ	0.3023 ℓ	0.1327 ℓ

Then, we obtain the per-unit-length impedance and admittance matrices as

$$\mathbf{Z} = \sum_{i=1}^6 \mathbf{Z}_i \ell_i / \ell \quad (12)$$

$$\mathbf{Y} = \sum_{i=1}^6 \mathbf{Y}_i \ell_i / \ell$$

and the procedure is similar as before. We obtain the approximated chain matrix by using (7), where Q_I , Q_{II} , Q_{III} and Q_{IV} correspond to the chain matrix calculated by using (12) for each line segment. After that we can obtain the approximated equivalent nodal matrix using (11).

C. Considering A Single Structure

Other possible approximation alternative consists in considering a single tower profile, i.e., the one with the largest length, as if it is the only configuration along the circuit. The natural ‘‘candidates’’ for this approach are those configurations that are dominant in the whole line, which in this case is configuration C_3 as it appear in almost 37% of the circuit length, and C_5 with roughly 30%. For each case, we obtain the approximated chain matrix by using (7), where Q_I corresponds to the chain matrix of 1/6 of the line total length obtained using either C_3 or C_5 as a single tower for the whole segment. Then $Q_{II} = Q_{III} = Q_I^2$ and $Q_{IV} = Q_I$ and, same as before, we use (11).

D. Comparison Between Approaches

In this section, $\mathbf{Y}_{n_{avg}}$ stands for the average approach described in Section III-B, and $\mathbf{Y}_{n_{C3}}$ and $\mathbf{Y}_{n_{C5}}$ stand for the approximated equivalent nodal admittance matrices calculated using only C_3 and only C_5 , respectively, following Section III-C. All possibilities for the admittance matrices are calculated from 0.01 Hz up to 50 kHz. For higher frequencies numerical issues are observed, due to the evaluation of the inverse matrices that are calculated when transforming the chain matrix into a nodal admittance matrix.

The magnitude of the elements in $\mathbf{Y}_{n_{eq}}$ together with the results obtained considering average impedances and admittances, only C_3 and only C_5 throughout the whole circuit are presented in Fig. 3. To highlight the differences, results

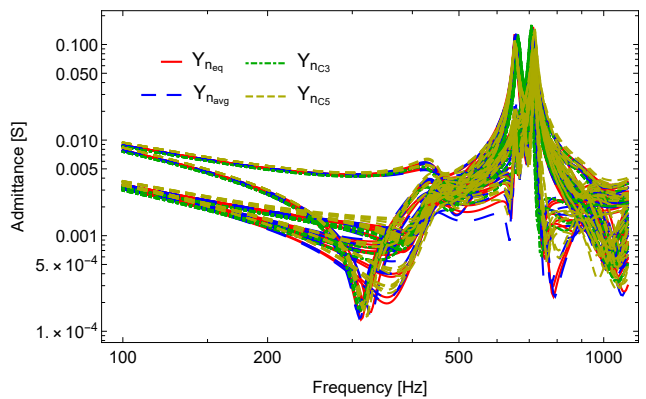


Fig. 3. Comparison of the behavior of the equivalent nodal admittance matrix and approximations.

are shown for a limited bandwidth. There are some small differences regarding the maxima in all three approaches, although the most noticeable differences are in the lowest values. These deviations can significantly impact the transient results. In Fig. 4 the behavior of the eigenvalues of the three approaches to the nodal admittance matrix is depicted. The main differences are for the eigenvalue with the highest damping (ground mode).

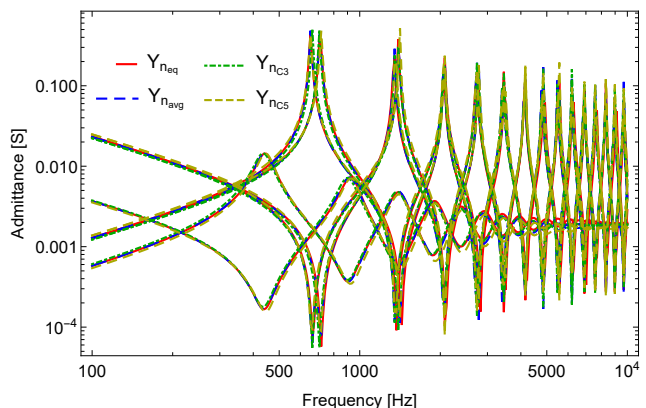


Fig. 4. Comparison of the eigenvalues of the equivalent nodal admittance matrix and approximations.

Figure 5 presents the deviation found between the approximate formulation and $\mathbf{Y}_{n_{eq}}$, they were calculated as

$$\begin{aligned} \Delta_1 &= \left| \mathbf{Y}_{n_{eq}} - \mathbf{Y}_{n_{avg}} \right| \\ \Delta_2 &= \left| \mathbf{Y}_{n_{eq}} - \mathbf{Y}_{n_{C3}} \right| \\ \Delta_3 &= \left| \mathbf{Y}_{n_{eq}} - \mathbf{Y}_{n_{C5}} \right| \end{aligned} \quad (13)$$

Besides the mismatches at the minima, some noticeable deviations can be found close to resonance peaks. It is worth mentioning that the uniform line based approaches present very similar performances throughout the frequency range of interest.

IV. TIME RESPONSES

For the assessment of time responses, we consider only a simple simultaneous three-phase energization test, as shown in

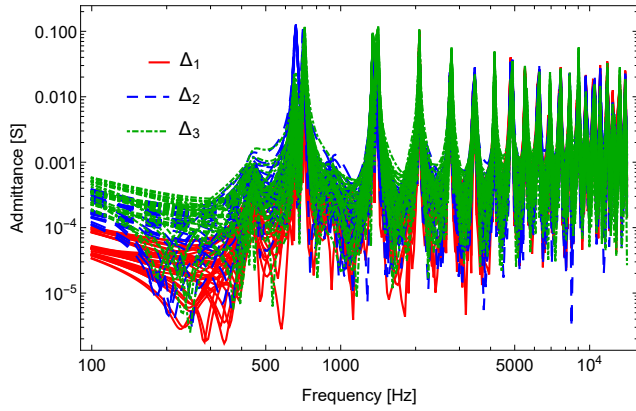


Fig. 5. Mismatches between \mathbf{Y}_{neq} and the approximated formulations.

Fig. 6, where SW_1 is an ideal three-phase breaker that closes at $t = 0$ s, SW_2 is a single-phase ideal breaker that also closes at $t = 0$ s. The short-circuit level at the sending end of the circuit is approximately 7.5 GW. The X/R ratio for the short-circuit equivalent is 50.

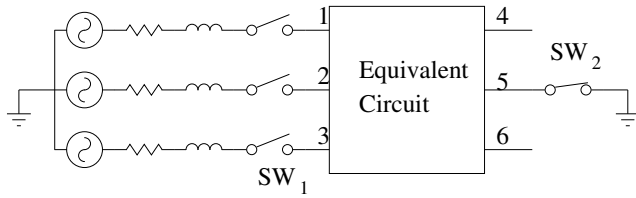


Fig. 6. Circuit for the time response test

To obtain the time response, we consider the Numerical Laplace Transform (NLT) [2,21]–[24]. We have considered 4096 frequency samples, and a total observation time of 100 ms. The total computation time was around 98 s. The network was implemented using the Wolfram Language and used the framework developed in [25].

Figure 7 depicts the voltage at node #4. All approaches provided similar results during the first time instants. However, while the approximation that considers average impedances and admittances remains close to the complete model, there is a rather noticeable difference when a single structure is considered for the whole circuit as the time progresses. Regardless of these deviations, \mathbf{Y}_{C_3} and \mathbf{Y}_{C_5} are rather close to each other.

If a direct energization is considered, i.e., SW_2 is assumed open during the simulation, the results presents a rather interesting situation as shown in Fig. 8. The peaks are more pronounced and occur in the first instants when \mathbf{Y}_{C_3} and \mathbf{Y}_{C_5} are considered.

Although not shown here, all the time responses were compared to a detailed representation of each C_i using the so-called Universal Line Model [13]. No significant mismatch was found when compared with the results obtained using \mathbf{Y}_{neq} . A disadvantage of this approach where each section of the circuit is represented lies in the fact that a short line length implies in the usage of an even shorter time-step limiting the largest time-step to be used in the simulation. The usage

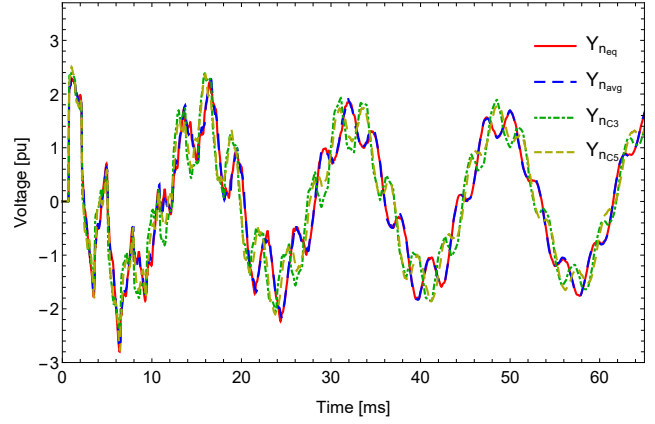


Fig. 7. Voltage response at node #4 considering all the possibilities to represent the nodal admittance matrix for the energization considering one phase at the receiving end in short-circuit.

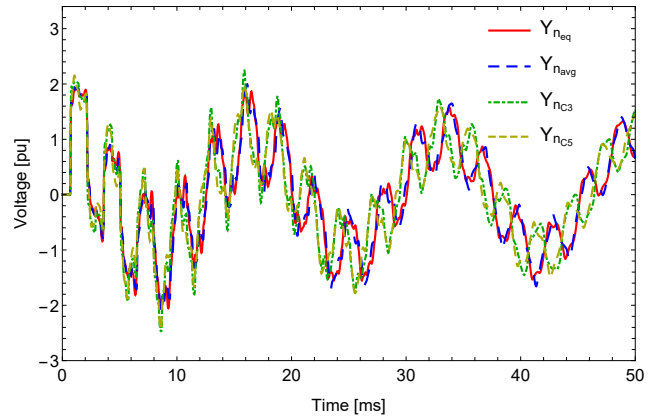


Fig. 8. Voltage response at node #4 considering all the possibilities to represent the nodal admittance matrix due to a simple energization.

of a rational approximation of \mathbf{Y}_{neq} tends to overcome this limitation. One could carry out the rational fitting of the equivalent nodal admittance matrix, which in most cases tends to have a poor resolution for weakly observable modes at lower frequencies, together with a rather large order equivalent. Some of these limitations can be overcome by resorting to a mode revealing transformation matrix (MRT) [26]. This procedure was applied recently to the rational approximation of the nodal admittance matrix of nonuniform lines [27].

V. CONCLUSIONS

This work investigated the impact of the usage of several distinct types of tower along a given circuit. The main reason for the investigation was due to the characteristics of the area where the circuit is expected to be built, which is a mountainous area, thus a large number of self-supporting towers is needed. This change in the geometric profiles causes a rather distinct characterization of the circuit when compared with the optimized configuration.

To improve the numerical performance of the overall system, a rather compact approach was used. It is based on the idea of defining a FDNE for the whole circuit. The FDNE was obtained using the chain matrix for the complete circuit.

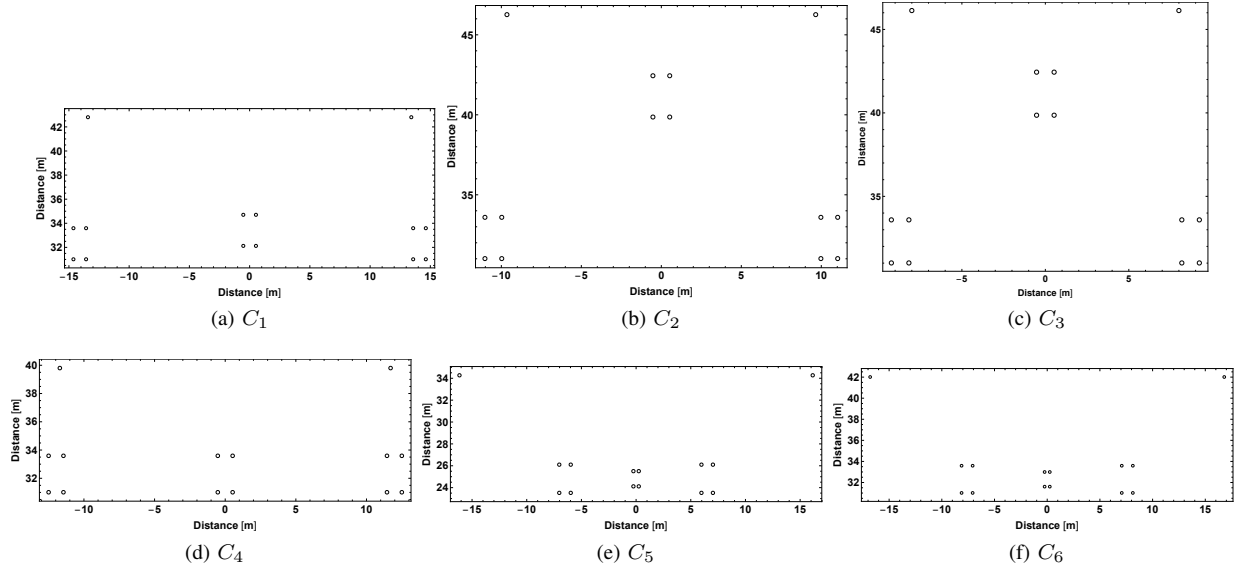


Fig. 9. Conductors arrangement considering the distinct structures (medium heights).

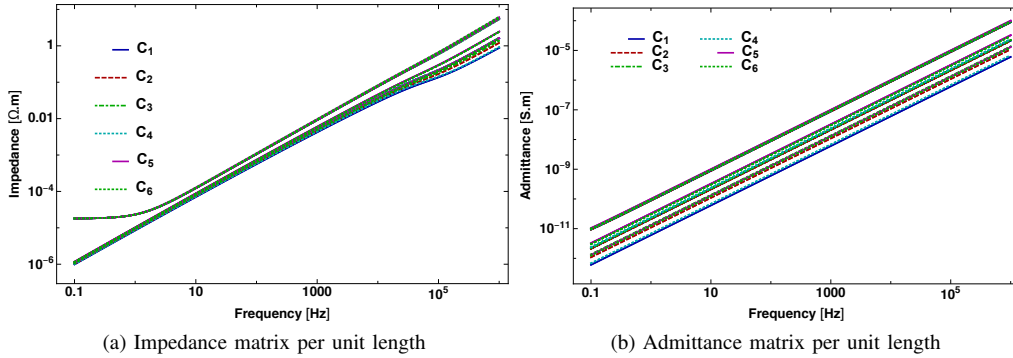


Fig. 10. Behavior of per-unit length parameters for the distinct C_i .

One issue with the FDNE is the limited bandwidth for the representation of the system. Due to the matrices inversion in the conversion of the chain matrix to the nodal admittance matrix, numerical error tend to arise at higher frequencies, typically near 100 kHz. Naturally, if the interest lies in high frequency phenomena, such as lightning performance, short line sections are to be of interest.

Simple formulations based on calculating average per-unit-length impedance and admittance for each segment, or using only one tower profile for the whole circuit are also investigated. It was found that these approximations tend to provide rather similar frequency domain profiles with the main differences in the lowest values and at the frequency where the highest values occur. While the average impedance and admittance approximation gives very close results to the complete model in both frequency and time domains, when a single tower profile is considered for the whole line, the small discrepancies in frequency cause some noticeable differences when time responses are considered.

APPENDIX

The several bundle arrangement used in the circuit are depicted in Fig. 9. There are configurations with only one type of bundle arrangement, i.e, C_1 to C_4 , while C_5 and C_6 show a central phase with a smaller bundle. The main difference between C_5 and C_6 lies in the average heights of the conductors. Figure 10 presents the behavior of the impedance and admittance matrices, both per unit length for the several configurations considered. It can be observed that for the impedance there are only small deviations in the mutual elements. Similar behavior is found for the admittance matrix, but in this case the deviations for the mutual elements are more pronounced.

REFERENCES

- [1] L. Wedepohl, "Application of matrix methods to the solution of the traveling-wave phenomena in poly-phase systems," *Proceedings of IEE*, vol. 110, no. 12, pp. 2200–2212, 1963.
- [2] L. M. Wedepohl and S. E. T. Mohamed, "Multiconductor transmission lines. theory of natural modes and Fourier integral applied to transient analysis," *Proceedings of the Institution of Electrical Engineers*, vol. 116, no. 9, pp. 1553–1563, 1969.

- [3] A. Semlyen and A. Dabuleanu, "Fast and accurate switching transient calculations on transmission lines with ground return using recursive convolutions," *IEEE Trans. on Power Apparatus and Systems*, vol. 94, no. 2, pp. 561–571, Mar. 1975.
- [4] A. Semlyen, "Contributions to the theory of calculation of electromagnetic transients on transmission lines with frequency dependent parameters," *IEEE Trans. on Power Apparatus and Systems*, vol. PAS-100, no. 2, pp. 848–856, Feb. 1981.
- [5] G. Angelidis and A. Semlyen, "Direct phase-domain calculation of transmission line transients using two-sided recursions," *IEEE Trans. on Power Delivery*, vol. 10, no. 2, pp. 941–949, April 1995.
- [6] F. Castellanos and J. Marti, "Phase-domain multiphase transmission line models," *Proceeding of IPST'95 – International Conference on Power Systems Transients*, vol. 1, no. paper 95IPST132-08, pp. 17–22, Sep. 1995, lisbon. [Online]. Available: www.ipstconf.org
- [7] T. Noda, N. Nagaoka, and A. Ametani, "Phase domain modeling of frequency-dependent transmission lines by means of an arma model," *IEEE Trans. on Power Delivery*, vol. 11, no. 1, pp. 401–411, Jan. 1996.
- [8] —, "Further improvements to a phase-domain ARMA line model in terms of convolution, steady-state initialization, and stability," *IEEE Trans. on Power Delivery*, vol. 12, no. 3, pp. 1327–1334, July 1997.
- [9] F. Castellanos, J. Martí, and F. Marcano, "Phase-domain multiphase transmission line models," *Electrical Power & Energy Systems*, vol. 19, no. 4, pp. 241–248, 1997, elsevier Science Ltd.
- [10] F. Marcano and J. Marti, "Idempotent line model: Case studies," in *Proceedings of IPST'97 - International Conference on Power Systems Transients*, 1997, pp. 67–72.
- [11] B. Gustavsen and A. Semlyen, "Calculation of transmission line transients using polar decomposition," *IEEE Trans. on Power Delivery*, vol. 13, no. 3, pp. 855–862, July 1998.
- [12] —, "Combined phase and modal domain calculation of transmission line transients based on vector fitting," *IEEE Transactions on Power Delivery*, vol. 13, no. 2, pp. 596–604, April 1998.
- [13] A. Morched, B. Gustavsen, and M. Tartibi, "A universal model for accurate calculation of electromagnetic transients on overhead lines and underground cables," *IEEE Trans. on Power Delivery*, vol. 14, no. 3, pp. 1032–1038, Jul. 1999.
- [14] L. Wedepohl and C. S. Indulkar, "Wave propagation in nonhomogeneous systems. Properties of the Chain Matrix," *Proc. IEE*, vol. 121, no. 9, p. 997, 1974.
- [15] B. Gustavsen, "Rational approximation of frequency dependent admittance matrices," *IEEE Transactions on Power Delivery*, vol. 17, no. 4, pp. 1093–1098, 2002.
- [16] —, "Computer code for rational approximation of frequency dependent admittance matrices," *IEEE Trans. on Power Delivery*, vol. 17, no. 4, pp. 1093–1098, Oct. 2002.
- [17] T. Noda, "Identification of a multiphase network equivalent for electromagnetic transient calculations using partitioned frequency response," *IEEE Trans. Power Delivery*, vol. 20, no. 2, pp. 1134–1142, Apr 2005.
- [18] R. Dias, A. Lima, C. Portela, and M. Aredes, "Extra long-distance bulk power transmission," *IEEE Trans. on Power Delivery*, vol. 26, no. 3, pp. 1440–1448, Jul. 2011.
- [19] C. Portela and M. Tavares, "Modeling, simulation and optimization of transmission lines. Applicability and limitations of some used procedures," in *Transmission and Distribution Conference*, 2002, invited paper.
- [20] A. C. S. Lima and C. Portela, "Inclusion of frequency-dependent soil parameters in transmission-line modeling," *IEEE Trans. on Power Delivery*, vol. 22, no. 1, pp. 492–499, Jan. 2007.
- [21] D. J. Wilcox, "Numerical Laplace Transformation and Inversion," *International Journal Elect. Eng.*, vol. 15, pp. 247–265, 1978.
- [22] F. A. Uribe, J. L. Naredo, P. Moreno, and L. Guardado, "Electromagnetic transients in underground transmission systems through the Numerical Laplace Transform," *Elsevier Electrical Power & Energy Systems*, vol. 24, pp. 215–221, 2002.
- [23] P. Moreno and A. Ramirez, "Implementation of the Numerical Laplace Transform: A review task force on frequency domain methods for EMT studies," *IEEE Trans. on Power Delivery*, vol. 23, no. 4, pp. 2599–2609, Oct. 2008.
- [24] P. Gomez and F. A. Uribe, "The Numerical Laplace Transform: An accurate technique for analyzing electromagnetic transients on power system devices," *International Journal of Electrical Power & Energy Systems*, vol. 31, no. 2-3, pp. 116–123, 2009. [Online]. Available: <http://www.sciencedirect.com/science/article/pii/S0142061508001002>
- [25] A. C. S. Lima, R. F. S. Dias, K. O. Salim, and M. T. Correia de Barros, "An open framework for lightning performance of overhead transmission lines," in *Lightning Protection (XIV SIPDA), 2017 International Symposium on*. IEEE, 2017, pp. 110–115.
- [26] B. Gustavsen, "Rational modeling of multiport systems via a symmetry and passivity preserving mode-revealing transformation," *Power Delivery, IEEE Transactions on*, vol. 29, no. 1, pp. 199–206, Feb 2014.
- [27] A. C. S. Lima, R. A. R. Moura, B. Gustavsen, and M. A. Schroeder, "Modelling of non-uniform lines using rational approximation and mode revealing transformation," *IET Generation, Transmission & Distribution*, vol. 11, no. 8, pp. 2050–2055, 2017.